Journal of Energy Storage 49 (2022) 104141

Contents lists available at ScienceDirect

Journal of Energy Storage

journal homepage: www.elsevier.com/locate/est

Research Papers

A computationally efficient adaptive online state-of-charge observer for Lithium-ion battery for electric vehicle

Bashar Mohammad Othman [a], Zainal Salam [a,*], Abdul Rashid Husain [a]

[a] Faculty of Engineering, School of Electrical Engineering, Universiti Teknologi Malaysia, Johor Bahru 81310, Malaysia

ARTICLE INFO

Keywords:
Adaptive observer
Computational cost
Lithium-ion battery
Lyapunov stability
State of charge

ABSTRACT

Due to the large number of cells installed in electric vehicle (EV), its battery management system (BMS) requires efficient state of charge (SOC) estimation algorithm. Since there is an impetus to reduce the computational burden (while retaining an acceptable accuracy), this paper proposes a simple and fast online adaptive observer for SOC estimation of Lithium-ion battery. The observer has several attractive features: first, its stability is proven by Lyapunov approach where asymptotic error convergence is guaranteed. Second, the computational requirements are low since it contains a few simple recursive equations without matrix inversion. Third, it is adaptive and achieves simultaneous online estimation of SOC and most of the battery parameters. The practical implementation using a 3 Ah battery proves the effectiveness of the proposed observer under dynamic stress test (DST). The testing with real EV profiles (supplemental federal test procedure which is known as US06 and federal urban driving schedule FUDS) is also performed to show the reliability. It is confirmed that the computation time of the proposed algorithm is reduced by approximately 2.5 times in compared to the extended Kalman filter-recursive least square (EKF-RLS) method. Despite the reduction in computation time, the errors are comparable to the latter. The low computational cost is significant when considering the need to accurately estimate the SOC of a large number of cells in a battery pack of an EV.

1. Introduction

The expected mass penetration of electric vehicle (EV) into the global automotive market will inevitably require drastic advancements in the battery management system (BMS). Since the battery pack is the most expensive component of the EV, it has to be operated at the highest efficiency, while retaining its safety features and longevity. The main function of BMS is to update the state of charge (SOC) of the battery so that the driver is continuously informed on the charge status—thus, removing the battery-depletion anxiety associated with EV driving [1]. Over the long term, the BMS also monitors the state of health (SOH) of the battery [2]. Other than these two main functions, the BMS needs to acquire, measure, condition and process the voltage, current and temperature signals, performs cell balancing, protects the battery pack and acts as interface with others electronics devices inside the vehicle.

By far, the SOC estimation is the most computational intensive operation for the BMS. The algorithm normally requires complex mathematical operations and dedicates a large portion of its computing resources for this purpose [2]. Although there exist low computation SOC algorithms such as the coulomb counting (CC) method, it lacks the necessary accuracy for EV application. The main problem with CC is the inherent accumulation error of the current integration. Furthermore, it mandates for an accurate initial value of SOC, which is an unknown variable in a real system [3]. A much more accurate estimation can be achieved using the artificial intelligence (AI) based SOC methods [4,5]. However, the system needs to be trained; this process is time consuming. Another drawback with AI is that, once the training is decided for a particular battery at a specific condition, it must be re-trained when operates in a different condition. This is not always feasible, considering the large variations in battery types and the highly dynamic nature of EV operations.

Thus far, the Kalman filter (KF) method is the most widely used SOC method. It estimates the battery state very accurately, even in the presence of noise. To deal with nonlinearity in the battery model, the improved KF, i.e. the extended Kalman filter (EKF) [6] and the sigma point Kalman filter (SP-KF) [7,8] are proposed. One of the main drawback of the KF-based methods is the need for an extensive computing power to perform a large number of matrix multiplications [2].

* Corresponding author.
E-mail address: zainals@utm.my (Z. Salam).

https://doi.org/10.1016/j.est.2022.104141
Received 7 June 2021; Received in revised form 13 December 2021; Accepted 30 January 2022
Available online 13 February 2022

Moreover, the EKF requires prior knowledge of the battery model's parameters before the estimation can be made. To obtain these parameters, additional procedures have to be incorporated into the original EKF algorithm. Two popular methods, namely the dual EKF (D-EKF) [9] and EKF with recursive least square (EKF-RLS) [10] are used; by this approach, the algorithm is able to estimate the state and the parameters simultaneously. Although the estimation performance is improved, the D-EKF and EKF- RLS require even more processing time to cater for these additional functions. Since the statistics of noise covariance are required in KF methods, an advanced adaptive EKF is proposed in [11] for online adaptation of the noise covariance and to solve the problem of filtering divergence caused by computer rounding errors.

The significance of the computational cost is crucial when BMS needs to monitor the SOC of the entire battery pack. To ensure optimal control, it is necessary to accurately estimate the SOC of each individual cell in the pack in real-time [12]. For example, the Tesla Model-S [13] pack consists of 7104 cells. Obviously, the determination of the SOC for individual cell can lead to massive computational requirement. Authors in [12] proposed the SP-KF to estimate the SOC using the "pack-average" method. Although, the BMS computational cost is reduced significantly, the error in the pack-average estimation is replicated to all other cells. Another approach is to estimate SOC for the critical cells only, i.e. the most and least charged cells. The SOC values of these cells basically determine how the entire battery pack should be charged or discharged [14]. However, the detection process of these critical cells is challenging and prone to error.

The main contribution of this paper is to propose SOC estimation method with low computational cost, thus it will be a good candidate for EV applications. Ideally, the best approach for the BMS in EV is to estimate the SOC of as many cells of the battery pack as possible. The more individual SOCs are known, the overall accuracy of the pack SOC is improved. However, this condition imposes a critical constraint on the BMS processing power. Thus, there is an impetus to reduce the computational cost of the SOC algorithm, while retaining an acceptable accuracy level. Hence, this paper utilizes the adaptive control theory to propose an online adaptive observer for SOC estimation of Li-ion. In [15], the author suggested a nonlinear observer with guaranteed stability based on Lyapunov theory. Despite the excellent performance for SOC estimation, the observer requires initial identification of the battery parameters prior to the SOC online estimation. This process has to be performed offline while the proposed observer combines the estimation of SOC and most of the battery parameters simultaneously. This type of observer has not been studied extensively for EV applications in literature. To the best of the author's knowledge, only the work in [16] applied the observer for battery parameters estimation under just one EV driving profile. The results are only presented for battery parameters without SOC result. While in [17] similar observer is presented for low excited currents only, thus there is a need for extended research of adaptive Lyapunov-based observer for EV application.

The adaptive Lyapunov-based observer [16,18] has several advantages: First, the stability is proven by Lyapunov. This implies that the observer is able to adapt to the change in the battery voltage. Second, the computational requirements are low since the observer contains a few simple recursion equations without matrix inversion. Third, it achieves simultaneous estimation of SOC and most of battery parameters. This is in contrast with the methods (for example EKF) which require all battery parameters to be known prior to the estimation. It also avoids the need for an additional online parameters estimation technique (for example D-EKF and EKF-RLS). Despite the low computing requirement, the proposed method exhibits comparable accuracy to the EKF-RLS. The proposed observer is tested with three EV profiles and shows reduction in the computational cost by approximately 2.5 times compared to the RLS-EKF method, while attaining close accuracy to the latter.

The paper is arranged as follows: In Section 2, the battery model is shown. The observer design is presented in Section 3, which contains the Lyapunov proof and systematic discretization of the observer which retains the Lyapunov properties. The experimental verification is shown in Section 4 and the algorithm validation under real driving profiles of EV is presented in Section 5. Finally, the computational cost evaluation of the proposed observer code shows the massive improvement in comparing with EKF-RLS code.

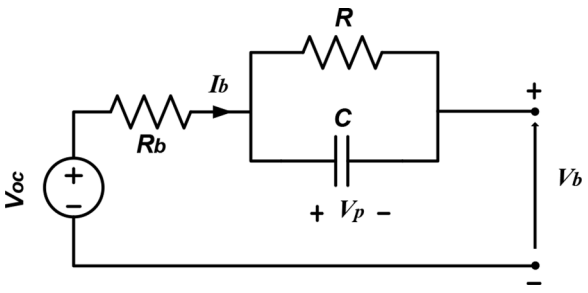

Fig. 1. The equivalent electrical model of a Li-ion battery.

2. Battery model

The SOC is defined as the ratio of the residual capacity to the total capacity of a battery [19]. In order to estimate the SOC, a dynamic electrical model is used. The popular single *RC* network model for the Li-ion battery is selected in this work, as shown in Fig. 1. It is much less complex than the double *RC* type [20], but exhibits sufficient accuracy, as concluded by Lai et al. [21]. Moreover, this model was used by numerous researchers, for example [22–24]. The state space representation of the model can be written as

$$\dot{V}_p = -\frac{1}{RC} V_p + \frac{1}{C} I_b \tag{1}$$

$$V_b = V_{oc} - V_p - R_b I_b \tag{2}$$

The battery current I_b is considered as the input of the model, while the battery voltage V_b is the output. The voltage across the *RC* network is the state. The model parameters are as follows: V_{oc}: open circuit voltage, R_b: series resistance, R: dynamic resistance, C: dynamic capacitor. Thus, voltage over R_b represents the instantaneous voltage drop, while the *RC* network simulates the diffusion of lithium. Since SOC is associated with V_{oc}, the observer aims to estimate V_{oc}; once this parameter is known, the SOC can be obtained by utilizing SOC-V_{oc} curve [25].

3. The proposed adaptive online observer

Most SOC algorithms utilize two-stage processes: initially an offline identification of battery parameters is performed; then, an online observer is used to estimate the SOC [26]. This approach does not consider the changes in the parameters; thus, the ageing factor (battery degradation) is not taken into account. Another approach is to perform a simultaneous online estimation for parameters and SOC using two observers [9]. Although this method is better, it needs to execute two separate procedures, namely the estimation of the model parameters and SOC concurrently. As a result, the computational requirement is much higher.

In this work, an improved online SOC estimation is proposed; it combines the estimation of model parameters values and V_{oc} (which is directly related to SOC) into a common equation. Thus, a single observer structure can be used to estimate the parameters and SOC simultaneously. It is important to note that the only prior knowledge needed is the time constant (τ) of the *RC* network. It is shown that this observer significantly reduces the computation without compromising on accuracy.

3.1. The observer design

The input/output relationship of model in Fig. 1 is obtained by substituting V_p from (2) into (1), i.e.

$$V_b = -RC\dot{V}_b - R_bRC\dot{I}_b - (R+R_b)I_b + V_{oc} + RC\dot{V}_{oc} \tag{3}$$

In the original paper published in [17], the derivative of the open circuit voltage ($\dot{V}_{oc}$) is assumed to be negligibly small; thus, $RC\dot{V}_{oc}$ is omitted. Although, this assumption is reasonable, its multiplication $\dot{V}_{oc}$ with RC enlarges the value of the term; consequently, the omission affects the accuracy. In this work, the $RC\dot{V}_{oc}$ is retained. Thus, V_b in (3) can be written as

$$V_b = \Phi^T W - \tau\dot{V}_b \tag{4}$$

where $W \in R^3$ is the model parameters vector, i.e.

$$W^T = [W_1\ W_2\ W_3] = [\tau R_b\ (R+R_b)\ (V_{oc}+\tau\dot{V}_{oc})] \tag{5}$$

and $\Phi\ \epsilon\ R^3$ represents the regressor vector, i.e.

$$\Phi^T = [-\dot{I}_b - I_b\ 1] \tag{6}$$

The reference model of the system is proposed as

$$\widehat{V}_b = \Phi^T\widehat{W} - \tau\dot{\widehat{V}}_b + \lambda\ e \tag{7}$$

and $\widehat{W} \in R^3$ is defined as the estimated model parameters

$$\widehat{W}^T = [\widehat{W}_1\ \widehat{W}_2\ \widehat{W}_3] = [\tau\widehat{R}_b\ (\widehat{R}_b+\widehat{R})\ (\widehat{V}_{oc}+\tau\dot{\widehat{V}}_{oc})] \tag{8}$$

The constant λ is the observer gain which is strictly positive, while e represents the estimation error, i.e. the difference between the actual and estimated voltage:

$$e = V_b - \widehat{V}_b \tag{9}$$

To make e converges to zero, i.e. asymptotic stability, the adaptation law is proposed as

$$\dot{\widehat{W}} = \Gamma.\Phi.e \tag{10}$$

where $\Gamma = [\Gamma_1\ 0\ 0;\ 0\ \Gamma_2\ 0;\ 0\ 0\ \Gamma_3]$ are positive adaptive gains to be selected.

3.1. The stability analysis

A stable SOC estimation is crucial for BMS because the battery is vulnerable to sensor's noise and occasional faulty readings. Such events can lead to estimation instability which eventually results in malfunction of the BMS. The proposed observer is designed based on Lyapunov stability which guarantees that the estimation error converges to zero. The following Lyapunov function is selected to attest the observer stability

$$V = \frac{1}{2}\left[\tau e^2 + \widetilde{W}^T\Gamma^{-1}\widetilde{W}\right]$$

where $\widetilde{W} = W - \widehat{W}$ is the difference between actual and estimated parameters. The first derivative of V yields

$$\dot{V} = \tau e\dot{e} - \widetilde{W}^T\Gamma^{-1}\dot{\widehat{W}} \tag{11}$$

Since the parameters in vector W are assumed to be slow time-varying [14], the following can be written

$$\dot{\widetilde{W}} = -\dot{\widehat{W}}$$

Substituting (10) in (11) yields

$$\dot{V} = \tau e\dot{e} - \widetilde{W}^T.\Phi.e \tag{12}$$

Adding and subtracting e^2 and substituting e from (9) yields

$$\dot{V} = e[V_b - \widehat{V}_b + \tau\dot{e} - e] - \widetilde{W}^T.\Phi.e \tag{13}$$

Setting the reference model $\widehat{V}_b$, as defined in (7), results in

$$\dot{V} = e\left[V_b - \Phi^T\widehat{W} + \tau\dot{\widehat{V}}_b - \lambda\ e + \tau\dot{e} - e\right] - \widetilde{W}^T.\Phi.e \tag{14}$$

Substituting V_b from (3) and $\Phi^T\widehat{W}$ from (6) and (8) yields

$$\dot{V} = e[-\tau\dot{V}_b - \tau R_b\dot{I}_b - (R+R_b)I_b + V_{oc} + \tau\dot{V}_{oc} + \tau\widehat{R}_b\dot{I}_b + (\widehat{R}_b+\widehat{R})I_b - \widehat{V}_{oc} - \tau\dot{\widehat{V}}_{oc} + \tau\dot{\widehat{V}}_b - \lambda\ e + \tau\dot{e} - e] - \widetilde{W}^T.\Phi.e \tag{15}$$

Further manipulation yields

$$\dot{V} = e[-\widetilde{W}_1\dot{I}_b - \widetilde{W}_2I_b + \widetilde{W}_3 - \lambda\ e - e] - \widetilde{W}^T.\Phi.e$$
$$\dot{V} = e\left[\Phi^T.\widetilde{W} - \lambda\ e - e\right] - \widetilde{W}^T.\Phi.e$$

which can be simplified to

$$\dot{V} = -e^2[\lambda + 1] \tag{16}$$

which yields $\dot{V} < 0 \forall e \neq 0$ Thus, $e = 0$is a globally asymptotically stable equilibrium point and the observer is asymptotically stable in the sense of Lyapunov.

It is important to realize that in addition to Lyapunov stability criteria, the persistence excitation (PE) condition must also be met [27]. This is to ensure proper excitation of battery model takes place, thus allowing the observer convergence to the correct value of the parameters. The PE is achieved if the input current contains a number of frequency components [28]. Fortunately for EV, the driving profiles (as presented later) suffice to meet the requirements of PE .

3.2. Observer discretization

For digital implementation, the continuous equations of the observer, i.e. (6) and (10) must be transformed into their discrete form. The discretized version reduces the computational cost because the codes can be customized without relying on the non-optimized C-codes generated by Simulink. Since the discretization need to maintain the Lyapunov stability criteria, the discrete form of (6) and (10) should have similar structure to continuous version. First, (7) is re-written as follows

$$\widehat{V}_b = -\tau\widehat{R}_b\dot{I}_b - (\widehat{R}_b+\widehat{R})I_b + \widehat{V}_{oc} + \tau\dot{\widehat{V}}_{oc} - \tau\dot{\widehat{V}}_b + \lambda e \tag{17}$$

Using difference equation, the discrete form of (17) can be written as

$$\begin{aligned}\widehat{V}_b(k) = {} & -\tau\widehat{R}_b(I_b(k) - I_b(k-1))/\ T_s - -(\widehat{R}_b+\widehat{R})I_b(k) + \widehat{V}_{oc}(k) \\ & + \tau(\widehat{V}_{oc}(k) - \widehat{V}_{oc}(k-1))/\ T_s - \tau(\widehat{V}_b(k) - \widehat{V}_b(k-1))/\ T_s \\ & + \lambda e(k-1)\end{aligned} \tag{18}$$

Note that, $e(k-1)$ is written instead of $e(k)$ since $e(k) = V_b(k) - \widehat{V}_b(k)$ is computed after finding $\widehat{V}_b(k)$. However, this modification can be accepted as the algorithm drops one sample of $e(k)$. This action does not affect the stability of the system since the dynamic of battery can be

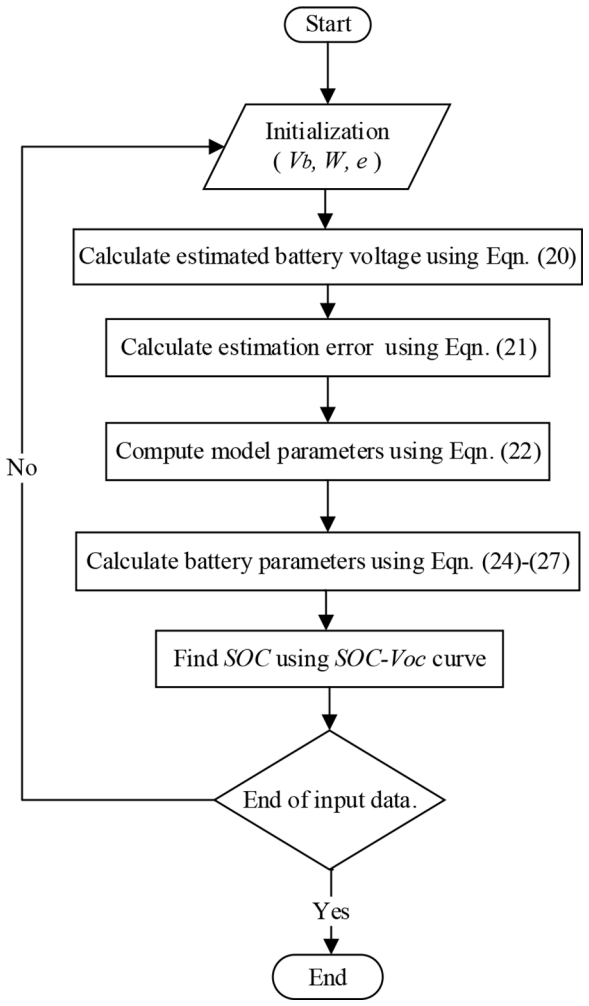

Fig. 2. . Flowchart of the proposed SOC algorithm.

considered as slow in comparison to other fuctions of the EV, for example speed control in the car. In the same way the estimated parameters can be written as

$$\hat{V}_b(k) = -\hat{W}_1(k-1)(I_b(k)-I_b(k-1))/\ T_s - \hat{W}_2(k-1)I_b(k) + \hat{W}_3(k-1) - \tau(\hat{V}_b(k)-\hat{V}_b(k-1))/\ T_s + \lambda e(k-1) \tag{19}$$

$\hat{V}_b(k)$ is moved to the left side of the equation, i.e.

$$\hat{V}_b(k) = \frac{1}{\tau + T_s}[\tau\ \hat{V}_b(k-1)\ -(\hat{W}_1(k-1) + T_s\hat{W}_2(k-1))I_b(k) + \hat{W}_1(k-1)I_b(k-1) + T_s\hat{W}_3(k-1) + T_s\lambda e(k-1)] \tag{20}$$

Thus, the estimation error in discrete form can be written as

$$e(k) = V_b(k) - \hat{V}_b(k) \tag{21}$$

The parameters adaption law (10) can also be discretized as follows

$$\hat{W}(k) = \hat{W}(k-1) + \Gamma.\hat{\Phi}\ (k).e(k).\ T_s \tag{22}$$

where $\hat{\Phi}\ (k)$ the regressor in discrete which can be derived from the

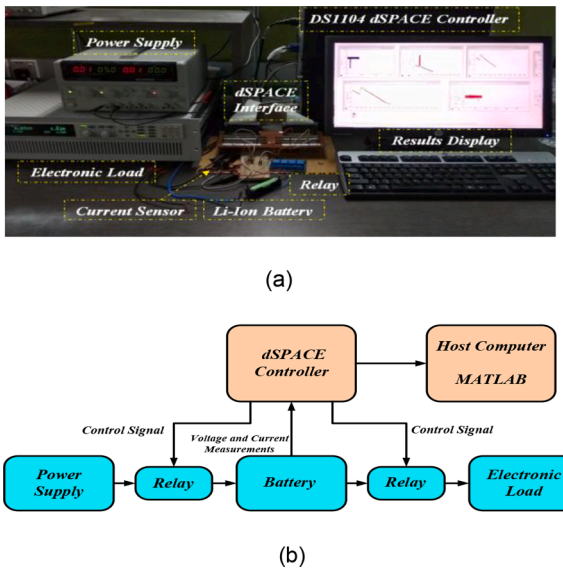

Fig. 3. The Experimental Test-Rig: (a) The Photograph of the Experimental Test-Rig. (b) The Block Diagram of Experiment.

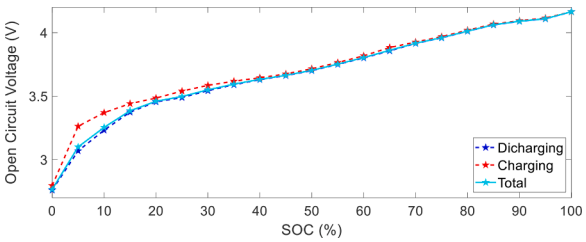

Fig. 4. SOC – V_{oc} relationship.

continuous regressor in (6).

$$\hat{\Phi}^{\ T}(k) = \left[\frac{-(I(k)-I(k-1))}{Ts}\ \ -I(k)\ 1\right] \tag{23}$$

Hence, the present value of $\widehat{W}$ will be substituted in (20) to calculate the next sample of $\hat{V}_b$. Meanwhile, the battery parameters are extracted from the Eq. (8), i.e.

$$\hat{R}_b = \frac{\hat{W}_1}{\tau} \tag{24}$$

$$\hat{R} = \hat{W}_2 - \hat{R}_b \tag{25}$$

$$\hat{C} = \frac{\tau}{\hat{R}} \tag{26}$$

$$\hat{V}_{oc}(k) = \frac{T_s}{\tau + T_s}\hat{W}_3 + \frac{\tau}{\tau + T_s}\hat{V}_{oc}(k-1) \tag{27}$$

The most important patameters is $\hat{V}_{oc}(k)$; once known, the SOC can be readily calculated using the relationship provided by the SOC versus V_{oc} curve of a specific battery [25]. The flowchart of the proposed algorithm is shown in Fig. 2.

Table 1
The Adaptive gain (Γ) and observer gain (λ) for DST profile.

Condition of SOC	Γ_1	Γ_2	Γ_3	λ
Above 20%	4	2.5	3	100
Below 20%	4	2.5	3	200

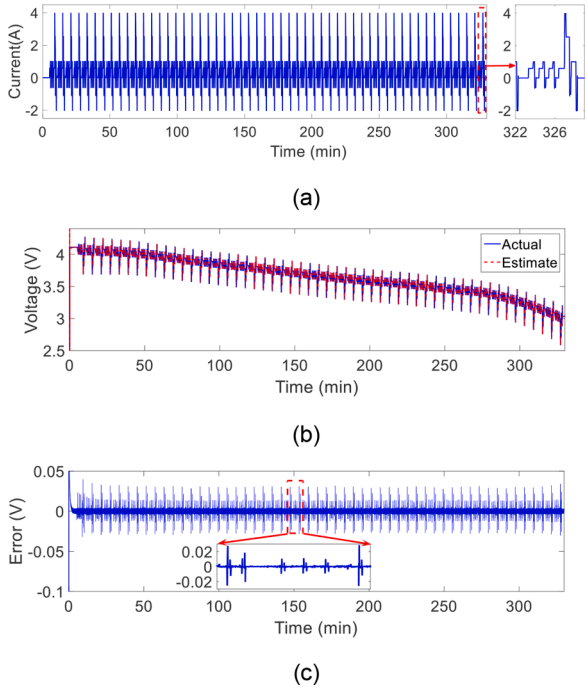

Fig. 5. (a) The current waveform of the DST (with inset) (b) actual and estimated voltage (c) voltage error.

4. Experimental verification

4.1. Test-rig set-up

The proposed online SOC method's effectiveness is validated using a 3 Ah Panasonic Li-ion battery (model NCR18650B). This battery is known as NMC since its positive electrode is made of nickel manganese cobalt oxide, while the negative electrode is graphite. An experimental test-rig is built, as shown in Fig. 3(a); it is based on the block diagram of Fig. 3(b). To evaluate the battery performance for EV, the dynamic stress test (DST) profile is used. The DST is a simplified version of the federal urban driving schedule (FUDS); since the charging and discharging profile of DST is much simpler than FUDS, the former can be implemented using the standard test equipment available at most laboratories [29]. The battery current is measured by a Hall effect sensor, while the voltage (less than 5 V) is measured directly (without a sensor). The DS1104 dSPACE controller is used to close the first relay (Fig. 3(b) and to open the second one in charging mode while it does the opposite for discharging, in accordance to the DST profile. Meanwhile, the controller also acts as a data acquisition interface unit—sending voltage and current signals to MATLAB, where the observer algorithm is implemented.

The SOC versus V_{oc} curve is determined using the incremental method [25]. Starting from a fully charged state (100% SOC), the battery is discharged at 0.5 C (1.5 A) for six minutes. Then it is left to relax for 54 min. At this point, the V_{oc} is measured; the recorded value is equivalent to 95% SOC. This process is repeated until the battery is fully discharged (0% SOC). The same procedure is carried out for the charging curve to charge the battery back to 100% SOC. Fig. 4 shows the discharging/charging curves. Since the charging curve is higher than the discharging, a hysteresis is noticed in the profile. However, since the hysteresis is very narrow (particularly beyond 20% SOC), it is neglected by considering the effective total curve which is calculated based on the 84:16 ratio of the DST profile. This ratio is derived from the amount of time allocated for discharging and charging, respectively. This makes sense, because in the real EV driving, the duration for charging is much lower. It is mostly obtained by regenerative braking.

Table 1a
Identified values of model and battery parameters using PSO.

	Model Parameters		Battery Parameters		
SOC (%)	*W1*	*W2*	R_b (ohm)	*R* (ohm)	*C* (Farad)
90	1.489	0.120	0.0856	0.0348	500.0
80	0.946	0.107	0.0801	0.0264	447.2
70	1.890	0.126	0.0772	0.0490	499.6
60	0.637	0.098	0.0774	0.0201	409.8
50	1.987	0.130	0.0700	0.0600	473.1
40	1.761	0.123	0.0730	0.0497	485.4
30	1.654	0.124	0.0771	0.0468	458.5
20	2.246	0.135	0.0753	0.0600	497.2
10	5.136	0.208	0.0879	0.1200	486.9
5	6.671	0.231	0.1112	0.1200	499.9

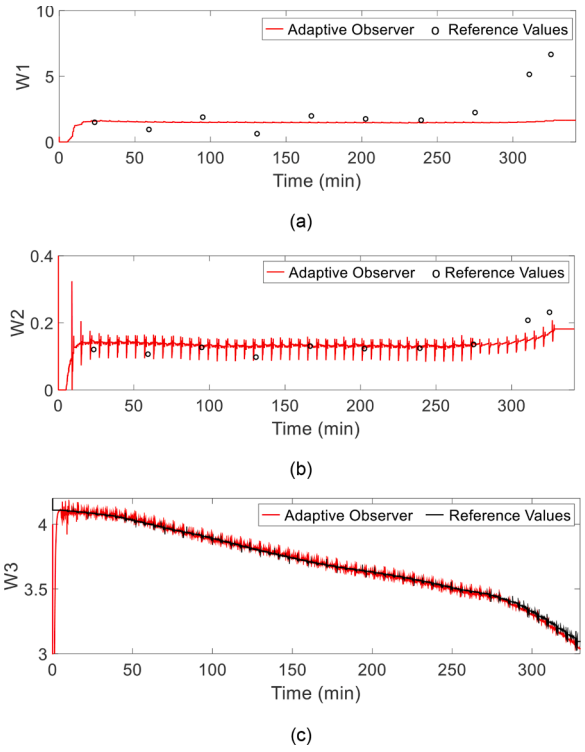

Fig. 6. Estimation of the model parameters of battery under DST profile (a) W_1; (b) W_2; (c) W_3.

The adaptive gain (Γ) and the observer gain (λ) are determined based on heuristic approach, and the selected values are shown in Table 1. There is tradeoff between convergence time and accuracy; large values of these parameters result in fast convergence. However, the accuracy is reduced because the effect of noise is amplified. It is important to note that when SOC goes below 20%, λ is set to higher value since the battery voltage and SOC have rapid changes at this range. To filter the noise in current and voltage signals, a low pass filter is added. The sampling time is set to 0.1 s.

4.2. Parameters estimation results

The DST consists of seven levels of discharging/charging DC current. The profile (and the enlarged inset) is shown in Fig. 5(a). The total

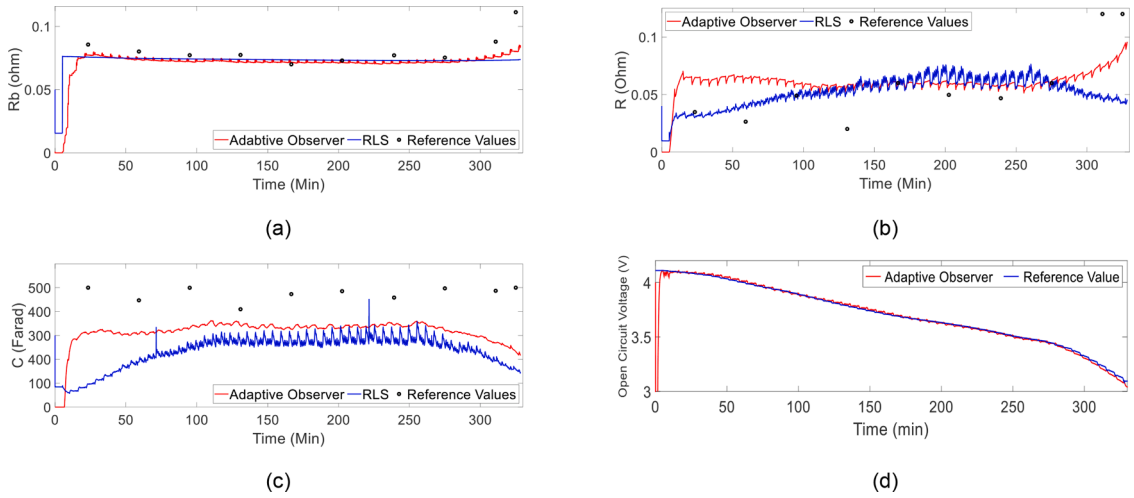

Fig. 7. Estimation of the battery parameters under DST profile (a) R_b; (b) R; (c) C; (d) V_{oc}.

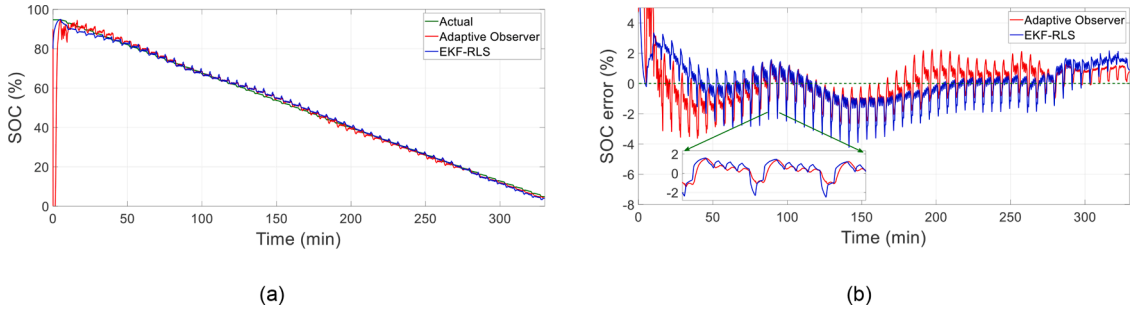

Fig. 8. The SOC estimation for DST driving profile (a) the SOC (b) the SOC error profiles.

duration for the driving cycle is 360 s. In the experiment, the profile is implemented for 328 min; this entire duration caused the SOC to drop from 95 to 5%. The observer estimates the battery voltage ($\widehat{V}_b$) to track the actual battery voltage (V_b). The estimation is based on Eq. (20). The profiles of $\widehat{V}_b$ and V_b under DST are shown in Fig. 5(b), while the error between the two profiles is shown in Fig. 5(c). It is seen that the observer estimates the voltage accurately. Since a steep transition characterizes DST's DC current steps, the error profile exhibits transitional spikes, as shown by the inset of Fig. 5(c). Meanwhile, the observer also updates the estimated model parameters $\widehat{W}$ based on (22). These values are substituted in (20) to calculate the next sample of $\widehat{V}_b$. Consequently, as $\widehat{V}_b$ is converging towards V_b, the estimated parameters $\widehat{W}$ is also converging to W.

To validate the estimation results of the model parameters by the observer, reference values of the tested battery are required. The particle swarm optimization (PSO) is utilized to find the model parameters W_1, W_2, then the reference values of the battery parameters i.e., R_b, R and C are computed by substituting in Eqs. (24)–(26). The reference value of V_{oc} (and hence W_3) is computed from the SOC versus V_{oc} curve Fig. 4. The objective (or cost) function for the PSO is the root square mean error (RMSE) between the actual battery voltage (V_b) and the output voltage by the model ($\widehat{V}_b$). The optimization process is carried out ten times (by increment of 10% SOC for each step). The identified parameters are shown in Table 1a.

The observer is able to estimate all model parameters ($W_1 - W_3$) without prior knowledge except the value of τ that is assigned to the observer prior to estimation. The observer achieves good estimation for model parameters as shown in Fig. 6 particularly for reference values corresponding to 90% to 20% SOC.

Using the previous estimated model parameters, the estimated battery parameters are calculated from (24) to (27). The results are shown in Fig. 7. To evaluate the performance of the proposed estimation method, it is benchmarked with the SOC technique, namely the EKF with recursive least square (EKF-RLS). The latter is re-implemented according to the procedures outlined in [30]. The advantage of the proposed adaptive observer is the simultaneous estimation of battery parameters, i.e., Fig. 7(a)–(c) and $\widehat{V}_{oc}$, i.e., Fig. 7(d). The result demonstrates the capability of the observer to track the changing values of $\widehat{V}_{oc}$ which decreases as the battery discharges. Finally, the values of $\widehat{V}_{oc}$ are translated to SOC using Fig. 4. On the other hand, the EKF-RLS is a two-step process. Initially, it predicts the next values of the system states. Then, it corrects the prediction using the measurements of the system's input and output signals. Unfortunately, these two steps involve extensive matrices multiplications, which consume a large portion of the BMS computational processing capacity [2]. Morover, EKF requires the values of battery parameters which are estimated by RLS as shown in Fig. 7 (a–c). The results from the RLS estimations are fed to EKF; only then the SOC can be estimated.

It is important to know that parameters convergence relationship is only in close approximation because the real judgement of the algorithm is based on the final SOC estimation where the actual SOC can be calculated accurately, then it can be used to evaluate the estimated SOC by both methods.

Table 2
The errors of the SOC estimation under DST.

Method	MAE%	RMSE%	Convergence Time (min)
Adaptive Observer	0.928	1.121	4.84
EKF-RLS	0.967	1.225	1.06

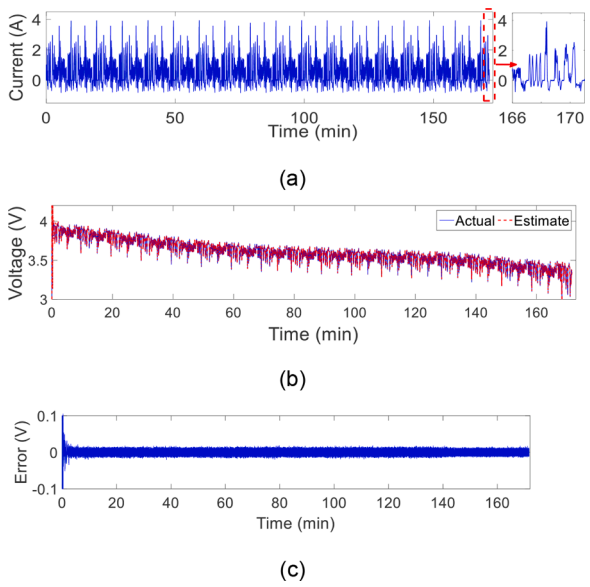

Fig. 9. (a) The current waveform of the US06 driving profile (with inset) (b) actual and estimated voltage (c) voltage error.

Table 3
The adaptive gain (Γ) and observer gain (λ) for the US06 and FUDS driving profiles.

Condition	Γ_1	Γ_2	Γ_3	λ
SOC above 20%	10	0.5	5	60
SOC below 20%	10	0.5	50	200

4.3. SOC estimation results

The estimated SOC values (of the DST profile) for the proposed observer and EKF-RLS are shown in Fig. 8(a). The reference SOC is determined by the calibrated coulomb counting approach [31]. The correctness of the reference SOC is ensured, since the actual capacity of the battery and the initial SOC values are known parameters. The SOC error profiles for both methods are shown in Fig. 8(b). The convergence time, which defined as the duration for the estimated value to stabilize within the 5% error bound, is used to assess the convergence ability. Furthermore, to quantify the accuracy, the mean absolute error (MAE) and the root mean square error (RMSE) are utilized. The performance of both estimators are summarized in Table 2. The proposed observer exhibits accuracies which are comparable to the EKF-RLS. This is noticed by the relatively similar MAE and RMSE values. The comparatively longer convergence time by the proposed observer is expected because both the battery model parameters and SOC must be estimated online simultaneously. The main advantage of proposed observer over EKF-RLS is in the computational cost; this is discussed in the last section. Moreover, the fulfilment of the Lyapunov stability criteria guarantees (in theory) the system stability. On the other hand, the system stability using EKF_RLS is not proven theoretically [9].

Table 4
The SOC estimation under US06 and FUDS driving profiles.

Profile	Method	MAE%	RMSE%	Convergence time (min)
US06	Adaptive observer	1.161	1.545	3.28
	EKF-RLS	1.45	1.789	12.6
FUDS	Adaptive observer	1.189	1.597	5.59
	EKF-RLS	2.059	2.266	0.47

5. Algorithm validation under real driving profiles

The adaptive observer is further tested using EV's real driving profiles: the supplemental federal test procedure which is known as US06 and FUDS schedules. The former is designed to simulate the highway driving, while the latter is for urban driving [29]. The tests are used to examine the battery performance by emulating the real patterns for EV driving, including discharging current during driving and charging current during braking. To implement the US06 and FUDS profiles on a battery, a special battery tester is required. Since this equipment is not available in our laboratory, the experimental data produced by the center for Advanced Life Cycle Engineering (CALEC), Universiy of Maryland, is utilized [32,33]. The CALEC data is acquired after implementing FUDS and US06 profiles on the 18650 Li-ion battery (rated at 2 Ah with NMC cathode material).

The US06 discharging and charging current profile is shown in Fig. 9 (a); the inset also shows the enlarged waveform. It consists of 17 cycles; each cycle is 600 s. Hence, the duration of the test is 170 min. On the other hand, the FUDS is applied continuously for eight cycles, where each cycle is 1372 s (total duration is 182 min), as shown in Fig. 11(a). By convention, the charging current is arbitrarily considered as a minus. It is noticed that FUDS exhibits higher charging current than US06 because the regenerative braking (which charges the battery) is more

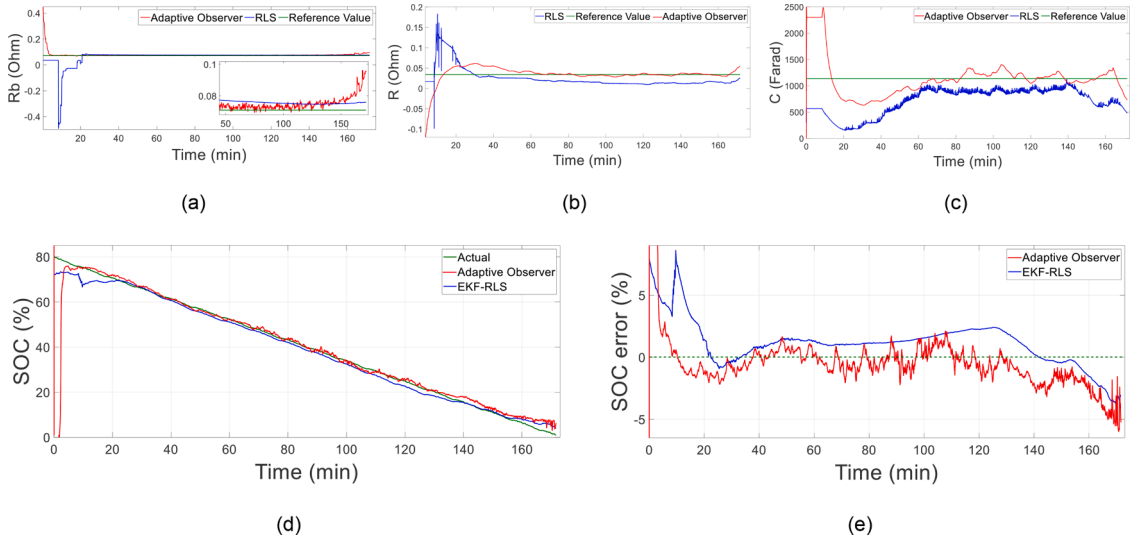

Fig. 10. The battery parameters and SOC estimation for US06 driving profile (a) R_b; (b) R; (c) C; (d) SOC; (e) SOC error.

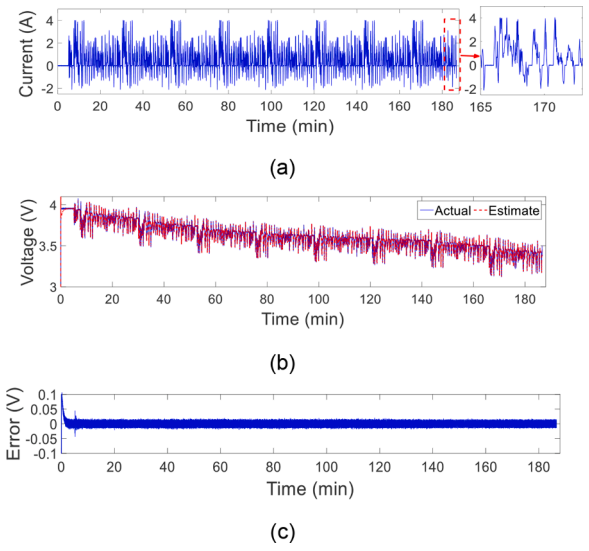

Fig. 11. (a) The current waveform of the FUDS driving profile (with inset) (b) actual and estimated voltage (c) voltage error.

prominent in urban driving. To simulate the practical working in EV, white noise is added to the voltage and current signals. The incorporation of this disturbance is needed because the data from CALEC is noise-free. The selected values of adaptive gain Γ and the observer gain λ are shown in Table 3 where the same gains are used to US06 and FUDS. The structure of the observer inherently adapts to the changes in the driving profile, without the need to change λ or Γ. When the SOC drops to below 20%, it is important to increase the Γ and λ as battery voltage and battery parameters change much more rapidly.

The profiles of the estimated ($\widehat{V}_b$) and actual (V_b) battery voltages for US06 are shown in Fig. 9(b), while the corresponding voltage errors are shown in Fig. 9(c). It is seen that the error is within ±10 mV, which indicates the good performance of the proposed observer.

The performance of the proposed observer and EKF-RLS for the US06 driving schedule are depicted in Fig. 10. The estimated battery parameters are shown in Fig. 10(a)–(c). The reference values of battery parameters are identified as fixed values by CALCE [33]. It is obvious that the estimated parameters by RLS exhibit overshoots thus, require more time to converge. On the contrary, the proposed adaptive observer shows improved performance; it requires shorter time for convergence. The estimated SOC and error profiles for both methods are shown in Fig. 10(d) and (e), respectively. As can be observed, the proposed observer shows better tracking for SOC and faster convergence time. The MAE and RMSE values are summarized in Table 4. The longer convergence time for EKF-RLS can be explained by the fact that the RLS takes longer time to estimate battery parameters for US06 profile.

The performance of the observer for FUDS profile is shown in Fig. 11. The main difference between US60 and FUDS is the high dynamic step change in current for the latter. As can be seen in Fig. 11(b), the estimated battery voltage ($\widehat{V}_b$) is tracking the actual voltage (V_b) well; the error is within ±10 mV as shown in Fig. 11(c). The estimated battery parameters are shown in Fig. 12(a)–(c). The SOC estimations by the proposed observer and EKF-RLS are depicted in Fig. 12 (d) and the SOC error for the both methods is shown in Fig. 12(e). The spikes exhibited by the proposed observer are due to the large current transition in FUDS profile (i.e. from -1.5 A charging to 4 A discharging). Thus, the observer requires time to converge to actual SOC.

The overall performance of both methods are summarized in Table 4. The estimated parameters by RLS have less accuracy than adaptive observer, particularly for the values of R (Fig. 12(a)–(c). These parameters result in less SOC accuracy by EKF-RLS comparing with adaptive observer (Table 4). On the other hand, the estimated parameters by adaptive observer are experiencing overshoots which result in longer convergence time for SOC comparing with EKF-RLS.

It is important to note that RLS-EKF is chosen as benchmark to

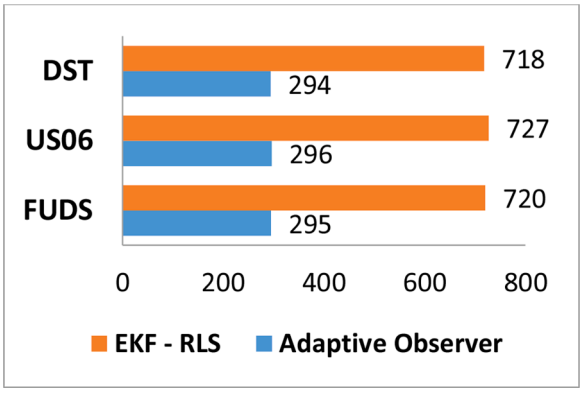

Fig. 13. Comparison of execution time (μs/sample) for the proposed adaptive observer and the EKF-RLS algorithm.

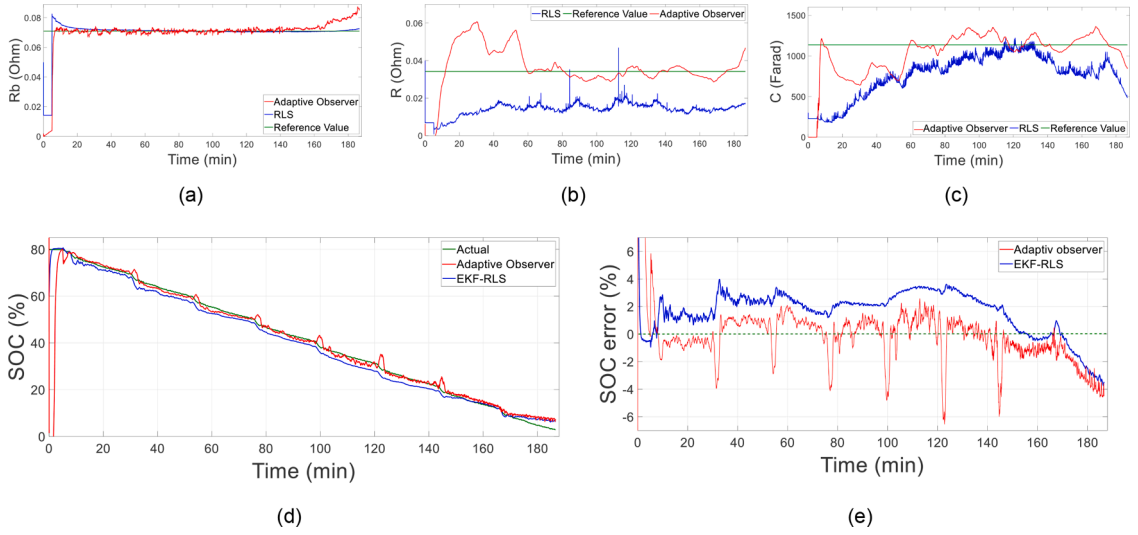

Fig. 12. The battery parameters and SOC estimation for FUDS driving profile (a) R_b; (b) R; (c) C; (d) SOC; (e) SOC error.

Table 5
Number of addition, multiplication and division for the competing SOC methods.

Method	Addition	Multiplication	Division	Total
Adaptive Observer	15	25	5	45
EKF-RLS	83	74	12	169

evaluate the trade-off between accuracy and computational cost. KF-based methods are the most commonly reported in the literatures which exist in many forms depending on the application. The advanced one like SP-KE can offer higher accuracy than EKF but with higher computational cost. Since this work focuses on reduction of computational cost, the benchmark with RLS-EKF is comparable as the proposed method achieves similar accuracy with effective reduction of computational time.

6. Computational cost evaluation

The main advantage of the proposed adaptive observer over EKF-RLS is the execution time of the algorithm. As stated earlier, the EKF consists of two main steps; each requires three sub-steps. For every step, many matrix multiplications are involved. Moreover, the RLS adds additional computational cost. On the other hand, the proposed method contains three simple recursive equations, i.e. (20), (22) and (27). Far less matrix multiplication is needed, and no matrix inversion is involved.

To quantify the computational execution time, both codes are run on PC (3.4 GHz CPU) with MATLAB 2015b. To determine the execution time per sample, each run's time is divided by the number of samples. The results are summarized in Fig. 13. As can be seen, the proposed observer is faster than EKF-RLS by approximately 2.5 times.

Moreover, the number of mathematical operations (i.e. addition, multiplication and division) are compared as shown in Table 5. The results clearly show the reduced number of operations needed for the adaptive observer. The main idea is to know which method has less computational requirements when applied on BMS. The shown results are considered as a guide for BMS designer. A powerful BMS can be chosen to estimate SOC for more cells in battery pack or alternatively, a cheaper BMS to estimate for few cells. However, in all cases and based on the computational cost evaluation, the adaptive Lyapunov-based observer offers less computational cost than RLS-EKF which gives BMS designer more options to do the trade-off between accuracy and cost of BMS. The computational cost reduction is very significant when considering large battery pack with massive number of cells. The low execution time reduces the heavy computation burden placed on the BMS processor.

6. Conclusion

The Lyapunov based adaptive observer is proposed in this paper. It is able to estimate SOC and most of the battery parameters concurrently with low computational requirements. In addition to guaranteed stability, the observer has simple structure—with only a few recursive equations. The experimental test on a 3 Ah battery using dynamic stress test (DST) proves the proposed observer's efficiency by achieving 0.928% mean absolute error. Moreover, it is tested using real EV driving profile (i.e. US06 and FUDS) and compared with EKF-RLS. The advantage of the proposed method is confirmed by reducing the computational cost by approximately 2.5 times compared to EKF-RLS, while attaining close accuracy. The overall excellent performance is envisaged to motivate the BMS designers to select the proposed observer as the SOC algorithm for the battery pack.

Authors statement

We confirm that this manuscript has not been published elsewhere and is not under consideration by another journal. All authors have approved the manuscript and agree with its submission to Journal of Energy Storage. We also confirm that the manuscript will not be published elsewhere in the same form, in English or in any other language, without the written consent of the Publisher.

Declaration of Competing Interest

The authors declare that they have no known competing financial interests or personal relationships that could have appeared to influence the work reported in this paper.

Acknowledgment

This research is supported by Yayasan Khazanah under the Khazanah Asia Scholarship Programme. The authors are also thankful to the Faculty of Engineering of Universiti Teknologi Malaysia for providing research facilities.

References

[1] S. Çeven, A. Albayrak, R. Bayır, Real-time range estimation in electric vehicles using fuzzy logic classifier, Comput. Electr. Eng. 83 (2020), 106577.
[2] M. Bingeman and B. Jeppesen, "Improving battery management system performance and cost with altera FPGAs," Altera Corporation, Jan, 2015.
[3] L. Lu, X. Han, J. Li, J. Hua, M. Ouyang, A review on the key issues for Lithium-ion battery management in electric vehicles, J. Power Sources 226 (2013) 272–288.
[4] M.A. A.wadallah, B. Venkatesh, Accuracy improvement of SOC estimation in Lithium-ion batteries, J. Energy Storage 6 (2016) 95–104.
[5] S. Tong, J.H. L.acap, J.W. P.ark, Battery state of charge estimation using a load-classifying neural network, J. Energy Storage 7 (2016) 236–243.
[6] S. Wang, C. Fernandez, L. Shang, Z. Li, H. Yuan, An integrated online adaptive state of charge estimation approach of high-power Lithium-ion battery packs, Trans. Inst. Meas. Control 40 (6) (2018) 1892–1910.
[7] W. Cao, S.L. Wang, C. Fernandez, C.Y. Zou, C.M. Yu, X.X. Li, A novel adaptive state of charge estimation method of full life cycling Lithium-ion batteries based on the multiple parameter optimization, Energy Sci. Eng. 7 (5) (2019) 1544–1556.
[8] S.L. Wang, C.M. Yu, C. Fernandez, M.J. Chen, G.L. Li, X.H. Liu, Adaptive state-of-charge estimation method for an aeronautical Lithium-ion battery pack based on a reduced particle-unscented Kalman filter, J. Power Electron. 18 (4) (2018) 1127–1139.
[9] C. Campestrini, T. Heil, S. Kosch, A. Jossen, A comparative study and review of different Kalman filters by applying an enhanced validation method, J. Energy Storage 8 (2016) 142–159.
[10] I. Jarraya, F. Masmoudi, M.H. C.habchoub, H. Trabelsi, An online state of charge estimation for Lithium-ion and supercapacitor in hybrid electric drive vehicle, J. Energy Storage 26 (2019), 100946.
[11] C. Jiang, S. Wang, B. Wu, C. Fernandez, X. Xiong, J. Coffie-Ken, A state-of-charge estimation method of the power Lithium-ion battery in complex conditions based on adaptive square root extended Kalman filter, Energy 219 (2021), 119603.
[12] G.L. P.lett, Efficient battery pack state estimation using bar-delta filtering, in: Proceedings of the EVS24 International Battery, Hybrid and Fuel Cell Electric Vehicle Symposium, 2009, pp. 1–8.
[13] M. Lelie, et al., Battery management system hardware concepts: an overview, Appl. Sci. 8 (4) (2018) 534.
[14] K.S.R. Mawonou, A. Eddahech, D. Dumur, E. Godoy, D. Beauvois, M. Mensler, Li-ion battery pack soc estimation for electric vehicles, in: Proceedings of the IECON 44th Annual Conference of the IEEE Industrial Electronics Society, IEEE, 2018, pp. 4968–4973.
[15] B. Xia, C. Chen, Y. Tian, et al., A novel method for state of charge estimation of Lithium-ion batteries using a nonlinear observer, J. Power Sources 270 (2014) 359–366.
[16] Y.H. Chiang, W.Y. Sean, J.C. Ke, Online estimation of internal resistance and open-circuit voltage of Lithium-ion batteries in electric vehicles, J. Power Sources 196 (8) (2011) 3921–3932.
[17] H. Chaoui, N. Golbon, I. Hmouz, R. Souissi, S. Tahar, Lyapunov-based adaptive state of charge and state of health estimation for Lithium-ion batteries, IEEE Trans. Ind. Electron. 62 (3) (2014) 1610–1618.
[18] J. Wei, G. Dong, Z. Chen, Lyapunov-based state of charge diagnosis and health prognosis for Lithium-ion batteries, J. Power Sources 397 (2018) 352–360.

[19] G.L. P.lett, Battery management systems, in: Equivalent-circuit Methods, Volume II, Artech House, 2015.
[20] M. Chen, G.A. R.incon-Mora, Accurate electrical battery model capable of predicting runtime and IV performance, IEEE Trans. Energy Convers. 21 (2) (2006) 504–511.
[21] X. Lai, Y. Zheng, T. Sun, A comparative study of different equivalent circuit models for estimating state-of-charge of Lithium-ion batteries, Electrochim. Acta 259 (2018) 566–577.
[22] J. Kim, J. Shin, C. Chun, B. Cho, Stable configuration of a Li-ion series battery pack based on a screening process for improved voltage/SOC balancing, IEEE Trans. Power Electron. 27 (1) (2011) 411–424.
[23] I.S. Kim, A technique for estimating the state of health of lithium batteries through a dual-sliding-mode observer, IEEE Trans. Power Electron. 25 (4) (2009) 1013–1022.
[24] J. Wei, G. Dong, Z. Chen, On-board adaptive model for state of charge estimation of Lithium-ion batteries based on Kalman filter with proportional integral-based error adjustment, J. Power Sources 365 (2017) 308–319.
[25] M. Petzl, M.A. D.anzer, Advancements in OCV measurement and analysis for Lithium-ion batteries, IEEE Trans. Energy Convers. 28 (3) (2013) 675–681.
[26] S. Muhammad, M.U. R.afique, S. Li, Z. Shao, Q. Wang, N. Guan, A robust algorithm for state-of-charge estimation with gain optimization, IEEE Trans. Ind. Inform. 13 (6) (2017) 2983–2994.
[27] B.M. Othman, Z. Salam, A.R. Husain, Analysis of online lyapunov-based adaptive state of charge observer for lithium-ion batteries under low excitation level, IEEE Access 8 (2020) 178805–178815.
[28] S. Boyd, S.S. S.astry, Necessary and sufficient conditions for parameter convergence in adaptive control, Automatica 22 (6) (1986) 629–639.
[29] C. Helen, D. Pat, D. Edward, Electric Vehicle Battery Test Procedures manual, Revision 2, Washington: US De-partment of Energy, 1996.
[30] I. Jarraya, F. Masmoudi, M.H. C.habchoub, H. Trabelsi, An online state of charge estimation for Lithium-ion and supercapacitor in hybrid electric drive vehicle, J. Energy Storage 26 (2019), 100946.
[31] D. Zhou, K. Zhang, A. Ravey, F. Gao, A. Miraoui, Online estimation of lithium polymer batteries state-of-charge using particle filter-based data fusion with multimodels approach, IEEE Trans. Ind. Appl. 52 (3) (2016) 2582–2595.
[32] CALCE, https://web.calce.umd.edu/batteries/data.htm.
[33] F. Zheng, Y. Xing, J. Jiang, B. Sun, J. Kim, M. Pecht, Influence of different open circuit voltage tests on state of charge online estimation for Lithium-ion batteries, Appl. Energy 183 (2016) 513–525.